Optofluidic in-fiber on-line ethanol sensing based on graphene oxide integrated hollow optical fiber with suspended core

DanhengGao[a], XinghuaYang[a,],PingpingTeng[a], DepengKong[b], ZhihaiLiu[a], Jun Yang[a], MengLuo[a], Zhanao Li[a], XingyueWen[a], LiboYuan[a,c], KangLi[d], NigelCopner[d]*

[a]Key Laboratory of In-Fiber Integrated Optics, Ministry of Education, College of Science, Harbin Engineering University, Harbin 150001, China

[b]State Key Laboratory of Transient Optics and Photonics, Xi'an Institute of Optics and precision Mechanic, Chinese Academy of Sciences, Xi'an 710119, China

[c]Photonics Research Center, Guilin University of Electronics Technology, Guilin 541004, China

[d]Nigel Copner are with the Wireless & Optoelectronics Research & Innovation Centre, Faculty of Computing, Engineering & Science, University of South Wales, Wales, CF37 1DL, UK

*yangxh@hrbeu.edu.cn

ABSTRACT: In this study, a novel in-fiber optofluidic trace ethanol sensor is proposed firstly. The microstructured hollow fiber (MHF) with a suspended core is a key part of the overall device which is integrated with graphene oxide (GO). The GO can be uniformly trapped on the whole surface of the suspended core in the MHF by using evanescent field inducing method. When trace microfluidic ethanol passes through the in-fiber device, the light intensity of the suspended core can be significantly modulated through the interaction between the GO on the core and ethanol. The device presents an excellent linearity on-line response with an average sensitivity of 0.16 dB/% with linear regression equation of y=0.16x+25.989. In general, this compact optofluidic in-fiber trace ethanol sensor can be utilized as for on-line detection of trace amounts of ethanol in special environments.

KEYWORDS: In-fiber device; Optofluidic sensor; Microstructured optical fiber; Graphene oxide

Carbon materials become a research hotspot due to their excellent electronic, magnetic, optical and thermal properties [1-3]. Especially, graphene is a very important kind of two-dimensional material. Generally, it is a two-dimensional hexagonal lattice of single-atom thick carbon materials composed of sp^2 bonded carbon atoms. Unlike graphene, graphene oxide (GO), as an oxidized form of graphene, contains many oxidizing functional groups, and these oxidizing functional groups greatly affect its electronic, mechanical, optical and electrochemical properties [4]. What's more, due to the functional groups on the surface of GO, especially the large amount of carboxyl groups and hydroxyl groups, it can be well combined with organic solvents in deionized water with rich negative charge. Recently, graphene oxide, as an important derivative of graphene, has been considered as an excellent alternative to graphene flakes, and has been widely applied in various areas including catalysis, biomedical, electrochemistry, and antimicrobial, especially in sensing applications [5-9].

Optofluidics as an emerging field is the combination of photonic and microfluidic technologies [10-12]. It is a tool that integrates sensing elements into a microfluidic device to generate an optical signal. This technology is very attractive in research fields such as sensing, chemistry, biomedical engineering, photonic devices [13-17]. On the other hand, microstructured hollow fibers (MHF) used as low loss waveguides and the microfluidic channel has shown unique advantages in constructing optical flow control sensors in fibers [18-20]. The small amount of fluid can flow through the MHF, because of the unique structure of the MHF. Meanwhile, a portion of the model field in the aperture allows the guided light to interact directly with trace amounts of sample through evanescent field effects. It makes use of the interaction between light and samples in microscale. In general, MHF is a natural optofluidic flow control carrier device [21-26].

In this paper, we integrate GO into a special designed MHF with suspended core and present an in-fiber on-line optofluidic device for trace ethanol detection. Specifically, adequate light can be coupled into the microfluid through the evanescent field of the suspended core within the bore of the MHF. The GO can be uniformly trapped on the whole surface of the suspended core in MHF by using evanescent field inducing. When trace microfluidic ethanol passes through the MHF, the signal intensity can be significantly modulated through the interaction between GO and ethanol [27-29]. Here, ethanol is widely used in food, daily necessities, and beverages [30, 31]. Excessive doses of ethanol can cause inflammation of the nasal mucosa and cause discomfort of skin. Therefore, it is essential for the detection of trace amounts of ethanol [32, 33]. In this paper, the in-fiber sensor based on GO film for ethanol detection has a high sensitivity and can be integrated with microreactor, micro-separators and other units.

METHODS

The sequential surface functionalization processes to coat the GO film schematically is shown in Fig.1. The piranha solution (4 volume of H_2SO_4 and 1 volume of H_2O_2) was injected into the MHF, and then the hydroxyl group was exposed. The inner surface of the MHF was hydroxylated. The exposed hydroxyl group (-OH) can be connected with the groups of the GO. Here, the concentration of GO solution was 0.5 mg/ml, and the absorption spectrum of GO is shown in Fig.2. The absorption peak of graphene oxide locates at 300-500 nm. So, we chose a coupling light wavelength of 485 nm. When the GO solution was filled into the MHF by capillary force, the semiconductor laser (3W maximum average power) was coupled into the fiber core from one end. Thus, the GO was coated onto the suspended core. In order to uniformly grow a robust graphene oxide film, the second part of the growth process needs to continuously couple the light for 20 minutes.

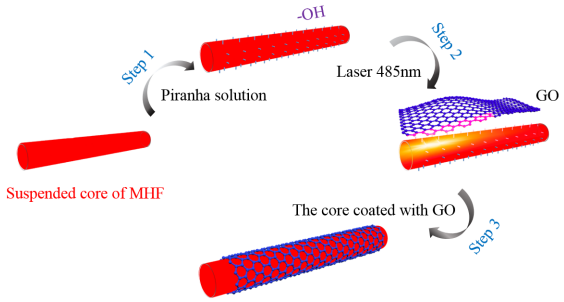

Fig.1. The fabrication procedure for the GO film deposition onto the suspended core in MHF for in-fiber optofluidic ethanol detection

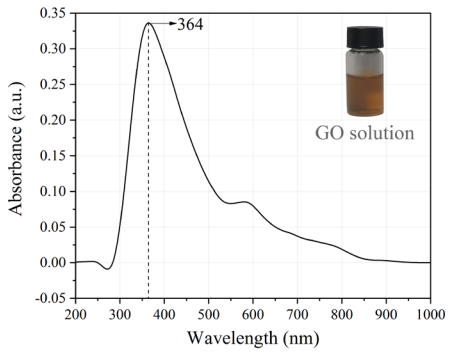

Fig.2. The absorption spectrum of the GO solution

The schematic diagram of the optofluidic in-fiber ethanol detection device with GO is shown in Fig.3. The proposed optofluidic MHF micro circulation channel is illustrated in the inset of the figure. The optofluidic part was composed of a piece of MHF modified with GO film. In particular, in the design, the MHF with an inner core based on silica was designed and fabricated in the lab. The microfluidic optical fiber was made by using tube and rod stacking method. Many parameters such as the heating temperature, translation speed, drawing speed and pressure in the hole were controlled during this process. By selecting suitable sets of parameters, we can completely control the profiles of the fibers. And the inset of the figure shows the cross-section of the MHF. The suspended core diameter is 8 μm, and its RI is 1.462. The diameter of the air hole in the MHF is 43 μm. And the thickness of the annular cladding with a RI of 1.472 is 41.5 μm. In addition, there is a suspended core inside the air hole of the MHF. During the grinding process for making microfluidic channel, the opening at the end face will not damage the structure of the core. The MHF grinding angle in the part of the air hole is about 15°. Meanwhile, the structure of the MHF is convenient to connect with single-mode fiber, which is convenient for light coupling. Both ends of MHF about 13 cm long were spliced with single mode fiber (SMF) by applying the electric arcs in a fusion splicer (Ji Long, KL-260B). In general, the optofluidic channel was built by grinding, polishing, and butt-jointing two ends of the MHF.

RESULTS AND DISCUSSION

Actual assembly of "SMF-input-MHF-output-SMF" is shown in inset of Fig.3. For the optical path, the suspended core of the MHF was coupled with the amplified spontaneous emission (ASE) light source and a spectrometer with a monochromator. 1550 nm was as chosen as the measure wavelength. And the light intensity at the wavelength was measured by an InGaAs2400-TE detector. Then, the light was coupled to the suspension core of the MHF through the SMF, and interacted with microfluidic sample of ethanol and GO through the evanescent field of the MHF core. To realize the optofluidic in-fiber ethanol detection, the sample solution was sucked through the microhole of the fiber by the negative pressure of the syringe pump and flows out from the other microhole of the fiber. Here, the different concentrations of ethanol solutions were obtained by mixing pure ethanol and deionized water in different ratios and the entire in-fiber optofluidic ethanol sensor is immobilized on a silica substrate with epoxy glue.

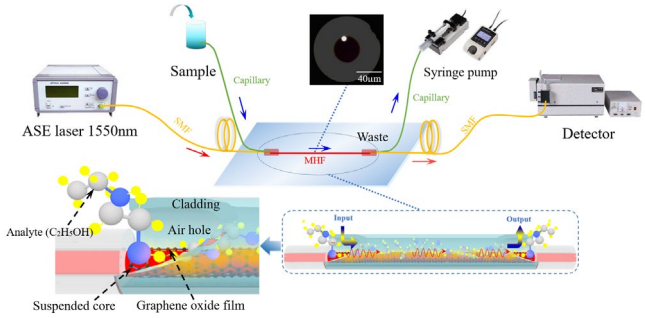

Fig.3. The diagram of the device for in-fiber optofluidic ethanol detection. Inset: end-face of MHF without growing GO film

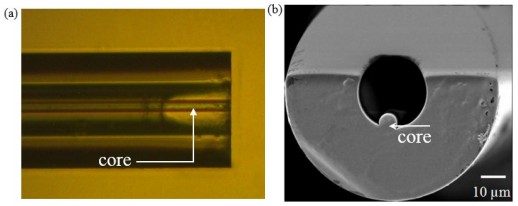

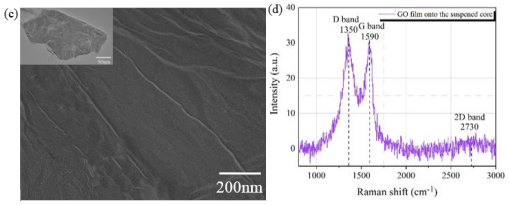

Fig.4. (a) The microscope image of the MHF without the GO film. (b) SEM image of end-face of the MHF with grown GO film. (c) SEM image of the GO film coated onto the surface of the core, inset the SEM of Go in solution. (d) Raman spectrum of the GO

Fig. 4(a) depicts the microscope image of the MHF after grinding. From this figure, the opened microhole at the fiber end is clearly observed, and the edge of the microhole is uniform. The suspended core can be seen inside and the structure is not damaged during the grinding process. The scanning electron microscope image (SEM-Hitachi S-3400N) at the end of the MHF is shown in Fig. 4(b), and it can be observed from the end face of the MHF that the GO film has been grown on the surface of suspended core. The surface morphology of the GO film on the surface of the core is further examined using a SEM, as exhibited in Fig.4(c). Its original morphology is in the form of sheet in the graphene oxide dispersion liquid like the inset of the Fig.4(c). When the GO solution is sucked into the fiber and the 485 nm laser is coupled, the GO solution forms a GO film on the suspension core under the action of a strong evanescent field of the fiber. From the figure, we can observe that the surface of the grown GO film is very complete and smooth. In general, GO can be successfully grown on the surface of the MHF suspended core by using the light-induced growth method.

Raman scattering spectroscopic characterization of the GO film coated on the suspended core of MHF excited with 532 nm laser is shown in Fig. 4(d). The spectral presents the typical D band at ~1350 cm^{-1} and the G band at ~1590 cm^{-1}. Hydroxyl groups and epoxy groups on the basal and local defects lead to the production of D bands, and the G band was formed due to the bond stretching of the sp^2 carbon pair in the ring and the chain. In general, the intensity ratio of I_{2D}/I_G for the 2D and G bands can characterize the number of layers of graphite material [34-36]. If the $I_{2D}/I_G < 0.7$, the GO is a single layer structure and if the $0.7 < I_{2D}/I_G < 1$, the GO is a double layer structure. When the $I_{2D}/I_G > 1$, the GO is a multilayer structure. In this experiment, $I_{2D}/I_G=0.1017$, this result shows that the GO is a single layer structure. Meanwhile, the thickness of the single graphene oxide layer should be about 0.8 nm and its refractive index was about 1.70 ± 0.30 [37]. Then, it can be confirmed the single layer structure GO can be smoothly and uniformly coated onto the suspended core.

In this device, the temporal intensity response at 1550 nm from the bare and GO-coated in-fiber optofluidic sensors is intuitively demonstrated in Fig. 5(a). And the Fig. 5(b) shows the relative optical intensity of each ethanol concentration in bare fiber and the GO-coated fiber. For the detection, we initially sucked the air (0% concentration of ethanol) into the microchannel of the MHF, and after a few minutes 20% (v/v) ethanol solution was inhaled, then 40% ethanol was taken, and so on. Fig. 5(a) presents the different concentrations of the microfluidic ethanol influenced the propagation of the light in the core. In particular, when the MHF was modified with Go, the collected outputs were greatly changed especially in the range of 80-100%. From Fig. 5(b), it can be seen throughout the measured range, GO-coated in-fiber optofluidic MHF is about 4.6 times more sensitive than the bare MHF for ethanol detection. This is because of the strong interaction between GO and the ethanol. The groups of the GO on the surface of the in-fiber optofluidic channel, such as -OH, -O- and -CO_2H, which combines with the -OH groups of ethanol to cause efficient adsorption of ethanol on GO under the action of a hydrogen bond network. In addition, the coating of graphene oxide also increased the evanescent field penetration depth of the suspended core. Thus, the GO significantly enhanced the sensitivity between optical fiber and target ethanol, consequently exhibiting a wide measurement range. As the volume fraction of ethanol increases, the absorption response of GO-coated fiber also increases. The result demonstrates that the in-fiber optofluidic channels of GO-coated can detect different concentrations of ethanol.

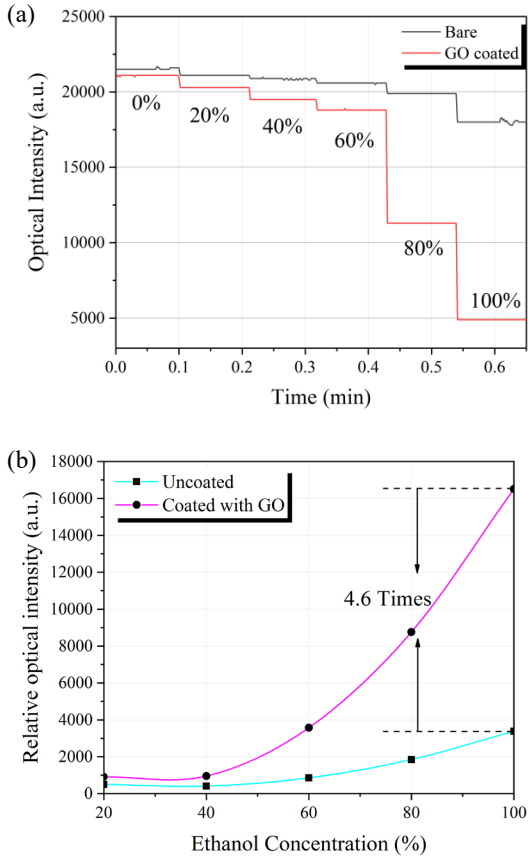

Fig.5. (a) Responses of the in-fiber optofluidic GO-coated MHF sensor and the bare fiber to ethanol with different concentrations. (b) Relative optical intensity changes with different concentrations

When the ordinate of Fig. 5(b) is transformed, the response of the device can be linearly regressed as Fig. 6. From the figure, the GO-coated in-fiber optofluidic MHF sensor exhibits its slope linearity of 99% shows a high sensitivity. The linear regression equation of the GO-coated MHF sensor can be expressed as $y=0.16x+25.989$ with the coefficient of $R^2=0.9947$, where y stands for the relative optical intensity and x is the ethanol concentration. The sensitivity of the GO-coated MHF is 0.16dB/%. Meanwhile, the ethanol concentration of 20%, 40%, 60%, 80%, 100%, the error analysis of multiple measurements is performed. From the error bar of the Fig. 6, the error of each concentration is very small. The maximum error

is only about 0.22 dB, which can explain that the device has a good reliability.

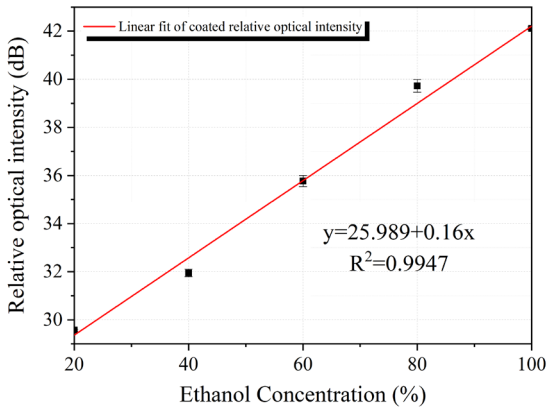

Fig.6. Linear fit of the responds to ethanol concentration for the in-fiber optofluidic sensor which is modified with GO sensing layer

To measure the stability of the GO-coated MHF optofluidic in-fiber sensor, different ethanol with the concentrations (20%, 40%, 60%, 80% and 100%) and air was alternately absorbed into the microfluidic channel. The corresponding dynamic responses of the device are depicted in Fig.7. For the response time, the device with GO can make a quick equilibrium when the sample pass through the fiber. The data from 0% to 20% ethanol concentration present that it is about 0.6 seconds which is shown in the inset. On the other hand, from the Fig. 7, the intensity value of the device when the air was absorbed remains substantially the same during each interval, which indicates that the device shows good stability.

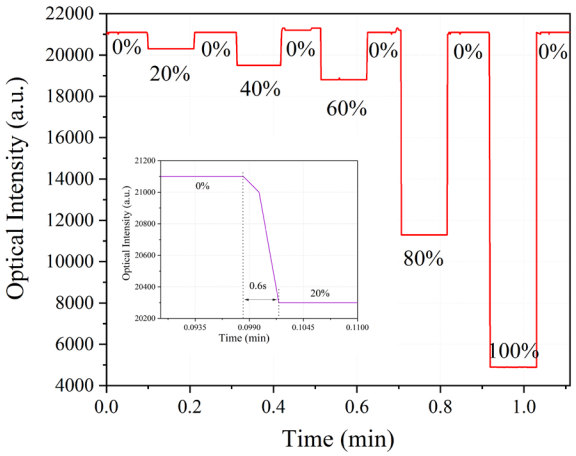

Fig.7. Dynamic response obtained for GO based in-fiber optofluidic MHF sensor towards ethanol

In order to examine the reliability of the developed sensors, sampling was done by repeatedly absorbing 80% of ethanol with random changes such as 40 % in the process, which is shown in Fig. 8. The results present the intensity change between the two sampling of the 80 % concentration is only 0.88 %. This indicate the interaction between GO and ethanol maybe a dynamic process. When the concentration around the core is the same, the bonding between GO and ethanol can reach a balance, which is of great significance for accurate quantitative detection of ethanol.

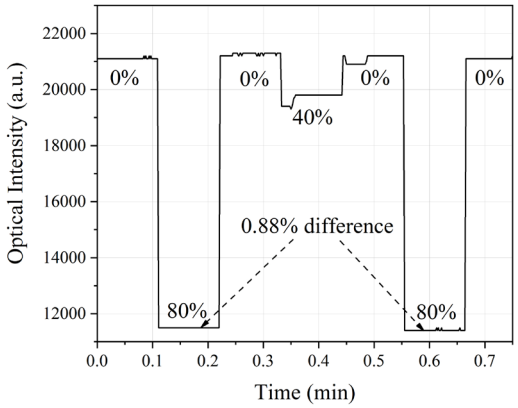

Fig.8. Repeatability of the GO based in-fiber optofluidic MHF sensor for alcohol detection

CONCLUSIONS

In conclusion, we first introduce GO into a special designed MHF with suspended core, and present an in-fiber integrated optofluidic device for ethanol detection. The GO film was deposited into the whole length of the MHF suspended core by using the MHF evanescent field. The device presents high sensitivity of ethanol detection because of the interaction of ethanol with GO in the fiber. Specifically, different concentrations of ethanol in the range of 0 to 100% in water can be online detected. The device shows a linearity response with an average sensitivity of 0.16dB/% with linear regression equation of y=0.16x+25.989. The experimental results show the in-fiber optofluidic device integrated with GO present high repeatability and stability to ethanol detection. It can be used for trace ethanol concentration analysis in many research fields such as food safety and environmental safety in the future.

AUTHOR INFORMATION

Corresponding Author

* E-mail: yangxh@hrbeu.edu.cn

Notes

The authors declare no competing financial interest.

ACKNOWLEDGMENT

This work is supported by the National Key R&D Program of China (2018YFC1503703); National Natural Science Foundation of China (NSFC, 11574061, 61405043); the Natural Science Foundation of Heilongjiang Province (LC2018026, F201405); the

Fundamental Research Funds for the Central Universities (3072019CF2502).

REFERENCES

1. Peng, Z.; Hu, Y.; Wang, J.; Liu, S.; Li, Ch.; Jiang, Q.; Lu, J.; Zeng, X.; Peng, P.; Li, F. Fullerene-Based In Situ Doping of N and Fe into a 3D Cross-Like Hierarchical Carbon Composite for High-Performance Supercapacitors. *Adv. Energy Mater.* **2019**, 1802928.

2. Li, D.; Müller, M. B.; Gilje, S.; Kaner, R. B.; Wallace, G. G. Processable aqueous dispersions of graphene nanosheets. *Nat. Nanotechnol*. **2008**, *3*, 101-105.

3. Liu, S.; Cui, L.; Peng, Z.; Wang, J.; Hu, Y.; Yu, A.; Wang, H.; Peng, P.; Li, F. Eco-friendly synthesis of N,S co-doped hierarchical nanocarbon as a highly efficientmetal-free catalyst for the reduction of nitroarenes. *Nanoscale* **2018**, *10*, 21764-21771.

4. Eda, G.; Fanchini, G.; Chhowalla, M. Large-area ultrathin films of reduced graphene oxide as a transparent and flexible electronic material. *Nat. Nanotechnol*. **2008**, *3*, 270-274.

5. Kim, H.; Cho, J.; Jang, S. Y.; Song, Y. W. Deformation-immunized optical deposition of graphene for ultrafast pulsed lasers. *Appl. Phys. Lett*. **2011**, *98*, 021104.

6. Toda, K.; Furue, R.; Hayami, S. Recent progress in applications of graphene oxide for gas sensing: *A review. Anal. Chim. Acta*. **2015**, *878*, 43-53.

7. Buelkea, C.; Alshamia, A.; Caslerb, J.; Linc, Y.; Hicknerd, M.; Aljundie, I. H. Evaluating graphene oxide and holey graphene oxide membrane performance for water purification. *J. Membrane Sci*. **2019**, *588*, 117195.

8. Basu, S.; Bhattacharyya, P. Recent developments on graphene and graphene oxide based solid state gas sensors. *Sens. Actuator B*. **2012**, *173*. 1-21.

9. Lee, J.; Kim, J.; Kim, S.; Min, D. H. Biosensors based on graphene oxide and its biomedical application. *Adv. Drug Deliv. Rev*. **2016**, *105*, 275-287.

10. Psaltis, D.; Quake, S. R.; Yang, Ch. Developing optofluidic technology through the fusion of microfluidics and optics. *Nature*. **2006**, *442*, 381-386.

11. Cooksey, G. A.; Patrone, P. N.; Hands, J. R.; Meek, S. E.; Kearsley, A. J. Dynamic Measurement of Nanoflows: Realization of an Optofluidic Flow Meter to the Nanoliter-per-Minute Scale. *Anal. Chem*. **2019**, *91*, 10713-10722.

12. Xiong, F.B.; Sisler, D. Determination of low-level water content in ethanol by fiber-opticevanescent absorption sensor. *Opt. Commun.* **2010**, 283, 1326-1330.

13. Fan, X.; White, I. M. Optofluidic Microsystems for Chemical and Biological Analysis. *Nat. Photonics*. **2011**, *5*, 591-597.

14. Schaich, M.; Cama, J.; Nahas, K.; Sobota, D.; Sleath, H.; Jahnke, K.; Deshpande, S.; Dekker, C.; Keyser, U. An Integrated Microfluidic Platform for Quantifying Drug Permeation across Biomimetic Vesicle Membranes. *Mol. Pharmaceutics*, **2019**, *16*, 2494-2501.

15. Zhao, Y.; Stratton, Z. S.; Guo, F.; Lapsley, M. I.; Chan, C. Y.; Lin, S. C.; Huang, T. J. Optofluidic imaging: now and beyond. *Lab Chip*. **2013**, *13*, 17-24.

16. Lin, C.; Liao, C.; Zhang, Y.; Xu, L.; Wang, Y. Fu, C.; Yang, K.; Wang, J.; He, J.; Wang, Y. Optofluidic gutter oil discrimination based on a hybrid-waveguide coupler in fiber. *Lab Chip*. **2018**, *18*, 595-600.

17. Yang, H.; Martin, A.; Gijs, M. Micro-optics for microfluidic analytical applications. Chem. Soc. Rev. 2018, 47, 1391.

18. Tai, Y.; Lee, C.; Chang, D.; Lai, Y.; Huang, D.; Wei, P. Escherichia coli Fiber Sensors Using Concentrated Dielectrophoretic Force with Optical Defocusing Method. *ACS Sens*. **2018**, *3*, 1196-1202.

19. Wang, Y.; Tan, X.; Jin, W.; Ying, D.; Hoo, Y. L.; Liu, S. Temperature-controlled transformation in fiber types of fluid-filled photonic crystal fibers and applications. *Opt. Lett*. **2010**, *35*, 88-90.

20. Ghaffar, A.; Liu, W. Y.; An, G.; Hou, Y.; Deeb, F.; Li, X.; Hussain, S.; Dharejo, F. A.; Zhang, H. X. A simple and cost-effective optical fiber angle measurement sensor using polymer optical fiber based on the TMBC. *Opt. Fiber Technol.* **2019**, 53, 102066.

21. Liu, S.; Gao, W.; Li, H.; Dong, Y.; Zhang, H. Liquid-filled simplified hollow-core photonic crystal fiber. *Opt. Laser Technol*. **2014**, *64*, 140-144.

22. Kaufman, J. J.; Tao, G.; Shabahang, S.; Banaei, E. H.; Deng, D. S.; Liang, X.; Johnson, S. G.; Fink, Y.; Abouraddy, A. F. Structured spheres generated by an in-fibre fluid instability. *Nature*. **2012**, *487*, 463-467.

23. Tai, Y.; Lee, C.; Chang, D.; Lai, Y.; Huang, D.; Wei, P. Escherichia coli Fiber Sensors Using Concentrated Dielectrophoretic Force with Optical Defocusing Method. *ACS Sens.* **2018**, *3*, 1196-1202.

24. Zhang, Y.; Ye, W. Q.; Yang, C. G. Simultaneous quantitative detection of multiple tumor markers in microfluidic nanoliter-volume droplets. *Talanta*. **2019**, *205*, 120096.

25. Wang, Y.; Wang, D.; Liao, C.; Hu, T.; Guo, J.; Wei, H. Temperature-insensitive refractive index sensing by use of micro Fabry-Pérot cavity based on simplified hollow-core photonic crystal fiber. *Opt. Lett*. **2013**, *38*, 269-271.

26. Yan, D.; Popp, J.; Pletz, M. W.; Frosch, T. Highly Sensitive Broadband Raman Sensing of Antibiotics in Step-Index Hollow-Core Photonic Crystal Fibers. *ACS Photonics*. **2017**, *4*, 138-145.

27. Fang, C.; Wu, H. Y.; Lee, S. Y.; Mahajan, R. L.; Qian, R. The ionized graphene oxide membranes for water-ethanol separation. *Carbon* **2018**, *136*, 262-269.

28. Zhan, W.; Xu, Z. J.; Yang, X. N. Molecular interlayer intercalation of ethanol-water mixture towards GO laminated membraned. *Sep. Purif. Technol.* **2019**, *233*, 116029.

29. Klechikov, A.; Yu, J.; Thomas, D.; Sharifi, T.; Talyzin, A. V. Structure of graphene oxide membranes in solvents and solutions, *Nanoscale* **2015**, *7*, 15374-15387.

30. Hu, P.; Du, G.; Zhou, W.; Cui, J.; Lin, J.; Liu, H.; Liu, D.; Wang, J.; Chen, S. Enhancement of ethanol vapor sensing of TiO2 nanobelts by surface engineering. *ACS Appl. Mater. Interfaces* **2010**, *2*, 3263-3269.

31. Cao, P.; Yang, Z.; Navalea, S. T.; Han, S.; Liu, X.; Liu, W.; Lu, Y.; Stadler, F. J.; Zhu, D. Ethanol sensing behavior of Pd-nanoparticles decorated ZnO-nanorod based chemiresistive gas sensors. *Sens. Actuator B*. **2019**, *298*, 126850.

32. Khan, S. B.; Rahman, M. M.; Akhtar, K.; Asiri, A. M.; Seo, J.; Han, H.; Alamry, K. Novel and sensitive ethanol chemi-sensor based on nanohybrid materials. *Int. J. Electrochem. Sci*. **2012**, *7*, 4030-4038.

33. Huang, R. R.; Liu, K.; Liu, H. J.; Wang, G.; Liu, T. H.; Miao, R.; Peng, H. N.; Fang, Y. Film-Based Fluorescent Sensor for Monitoring Ethanol-Water-Mixture Composition via Vapor Sampling. *Anal. Chem*. **2018**, *90*, 14088-14093.

34. Poncharal, P.; Ayari, A.; Michel, T.; Sauvajol, J. L. Raman spectra of misoriented bilayer graphene. *Phys. Rev. B* **2008**, 78, 113407.

35. Bouša, M.; Frank, O.; Jirka I.; Kavan, L. In situ Raman spectroelectrochemistry of graphene oxide. *Phys. Status Solidi B* **2013**, 12, 2662-2667.

36. Hu, Y.; Ma, H.; Liu, W.; Lin, Q.; Liu, B. Preparation and Investigation of the Microtribological Properties of Graphene Oxide and Graphene Films via Electrostatic Layer-by-Layer Self-Assembly. *J. Nanomater.* **2015**, 10, 1-8.

37. Inhwa J.; Matthias V.; Matthew P.; Richard P.; Dmitriy A. D.; Sasha S.; Jinho A.; Rodney S. R. Characterization of Thermally Reduced Graphene Oxide by Imaging Ellipsometry. *J. Phys. Chem. C* **2008**, *112*, 8499-8506.